

**TIME-DOMAIN MODELING OF WIRELESS POWER TRANSFER IN MOTION USING
INDUCTIVELY COUPLED FLAT SPIRAL COILS**

A thesis presented to the faculty of the Graduate School of Western Carolina University in
partial fulfillment of the requirements for the degree of Master of Science in Technology

By

Joshua Nathan Turnbull

**Director: Dr. Bora Karayaka
Associate Professor
School of Engineering and Technology**

Committee Members:

**Dr. Robert Adams School of Engineering and Technology
Dr. Andrew Ritenour School of Engineering and Technology
Dr. Weiguo Yang School of Engineering and Technology**

November 2020

This work is dedicated to those I have lost during my college journey:

My father Kevin Turnbull, my great grandfather Tony Hacker

my best friends Ashley Gilley and Kayla Duquette,

my great aunts Sheila Syrett, Jennifer Jacobs, Bonnie Erbacher, and Jonita Jacobs.

Also, to those that kept me going through the pain and have provided more than I can repay:

My mother and her husband, Elisa and Andrew Rogers,

and the Fieret, Gilley, Snyder, and Wells families

ACKNOWLEDGEMENTS

I want to thank and acknowledge the professors and staff of Western Carolina University's School of Engineering and Technology and their endless understanding, support, and encouragement. Dr. Paul Yanik for helping me make the choice to attend graduate school at WCU, considering me for assistantships, and pushing me at each turn. Dr. Peter Tay for breaking apart subjects that I find very difficult into things I can understand, helping me work on my coding skills, which had been my weakness, and increasing my drive to be a well-rounded engineer. Dr. Weiguo Yang and Dr. Andrew Ritenour for making me curious about fields and technologies in engineering that I did not know existed and for being great soundboards for my many ideas. Dr. Bora Karayaka, for taking on my thesis, understanding my passion, helping me stay focused, and being very understanding of the issues I was facing. WCU's School of Engineering and Technology went above and beyond and helped me succeed through many significant life events, and I am forever grateful.

I would also like to thank my family and friends for always being there and sticking together, and growing closer in our times of loss, uncertainty, and crisis. I thank Premkumar Subbukutti, Tanmay Shohel, Anik Tahabilder, AJ Mongold, Kent Wheless, Adrian Correa, Brittany Nelson, Taryn Barefoot, and my lifetime friend Patrik Gilley for making my time much more enjoyable and fulfilling. Special thanks to Ian Green for joining thesis meetings, adding to the conversation and information, and keeping me focused.

TABLE OF CONTENTS

ACKNOWLEDGEMENTS	iii
TABLE OF CONTENTS.....	iv
LIST OF FIGURES	vi
ABSTRACT.....	vii
CHAPTER 1: INTRODUCTION.....	1
1.1 Problem Statement	1
1.2 Background	3
1.3 Thesis Objectives and Scope.....	4
CHAPTER 2: LITERATURE REVIEW	6
2.1 Background	6
2.2 Coil Design and System Modeling Optimization	7
2.3 Issues	8
2.5 Benefits to Proposal	8
CHAPTER 3: METHODOLOGY AND DESIGN.....	10
3.1 Modeling the Coils and Circuit	10
3.2 Modeling Mutual Inductance	16
3.3 Modeling the System in Simulink® and MATLAB®	17
3.4 Modeling a System with Multiple Transfer Coils.....	24
3.5 Model Modification for Understanding Effects of Variables on the System.....	26
CHAPTER 4: RESULTS	28
4.1 General Testing Results	28
4.2 Identical Transmitting and Receiving coil	29
4.3 Non-Identical Transmitting and Receiving coil	34
CHAPTER 5: CONCLUSION AND FUTURE WORK.....	40
5.1 Conclusion.....	40
5.2 Future Work and Considerations.....	41
REFERENCES	43
APPENDICES	45
Appendix A Source Code.....	45
Appendix B Example of Excel Calculation Sheet	48
Appendix C Output Power Values for Identical Coils.....	49

Appendix D Output Power Values for Non-Identical Coils 50

LIST OF FIGURES

Fig. 1. Measurements for a Spiral Coil	10
Fig. 2. Series-Series Compensated WPT Circuit	12
Fig. 3. Reduction of WPT Circuit Using a Thevenin Equivalent Circuit	13
Fig. 4. Graphical Representation of the Equivalency of the Coil Spacing	18
Fig. 5. Graphical Representation of Full Spacing	19
Fig. 6. Mutual Inductance for Identical Coils Using Default Parameters.....	21
Fig. 7. Block Diagram of the System Modeled in Simulink®.....	22
Fig. 8. Phase Variable Canonical Form Simulation Block Internal.....	23
Fig. 9. Output Voltage of a Two Transmitter Coil System with Identical Coils	25
Fig. 10 Effect of Load Resistance on the Output Voltage Waveform of Identical Coils	29
Fig. 11. Affect of Frequency on Output Power for Identical Coils	30
Fig. 12. Affect of Speed on Output Power for Identical Coils	31
Fig. 13. Affect of Load Resistance on Output Power for Identical Coils	32
Fig. 14. Affect of Y-Offset on Output Power for Identical Coils	33
Fig. 15. Affect of Z-Offset on Output Power for Identical Coils	34
Fig. 16. Affect of Frequency on Output Power for Non-Identical Coils	35
Fig. 17. Affect of Speed on Output Power for Non-Identical Coils	36
Fig. 18. Affect of Load Resistance on Output Power for Non-Identical Coils.....	37
Fig. 19. Affect of Y-Offset on Output Power for Non-Identical Coils.....	38
Fig. 20. Affect of Z-Offset on Output Power for Non-Identical Coils	39

ABSTRACT

TIME-DOMAIN MODELING OF WIRELESS POWER TRANSFER IN MOTION USING INDUCTIVELY COUPLED FLAT SPIRAL COILS

Joshua Nathan Turnbull, M.S.T.

Western Carolina University (November 2020)

Director: Dr. Bora Karayaka

In current commercial technologies, wireless power transfer (WPT) occurs when the item charging and the charger are not in motion. Products such as wireless chargers for cell phones, cars, and some internet of things (IoT) devices have stationary wireless chargers. A limiting factor of these chargers is in a single transfer coil system, the coils need to be aligned perfectly, and the device must be physically touching the charger. If it is not, minimal or no power is transferred, and the device is not charged. This set-up allows manufacturers to simplify design and modeling as a steady-state system. In this thesis, the receiving coil is in motion over the embedded transfer coil. The industrial standard to discern how the system would react uses finite element analysis (FEM), which is very resource-intensive and time-consuming. The point of this thesis is to model and approximate the potential of a WPT system to help discern the viability of designs, therein reducing the number of resources and time necessary to find an optimum solution. A Series-Series Compensated Wireless Power Transfer circuit was solved using Thevenin Equivalent Circuits and converted into a state-space equation. Using MATLAB® and Simulink, the circuit was modeled and compared to another study to validate the results. Variables such as frequency, load resistance, vertical and horizontal offset were then changed to

see how the output voltage waveform and power transfer changed. Due to the receiving coil's motion, a steady-state is not reached, and the system has transient states. The effects on the waveforms, thoughts about optimization, and possible future studies are discussed.

CHAPTER 1: INTRODUCTION

1.1 Problem Statement

Climate change is a term that is frequently thrown around and just as frequently not quantified or fully explained as such many do not understand the gravity of the situation. The earth goes through warming and cooling cycles due to balances of different greenhouse gases in the atmosphere and solar radiation bouncing off reflective surfaces on earth. Usually, 35% of solar radiation is reflected into space by the atmosphere, 18% is trapped in the atmosphere, and 46% is absorbed by the earth [1]. However, when the earth is in a warming cycle, an increased percentage is trapped in the atmosphere, which begins to drive a positive feedback loop. An increased amount of greenhouse gasses like CO₂, water vapor, and nitrous oxide causes this increase.

CO₂ is the driving force of climate change, not due to its ability to capture solar radiation, but because of the sheer amount of CO₂ in the atmosphere. CO₂ accounts for 80% of the contribution of the greenhouse gasses to climate change [2]. In 2017 humans emitted 36 Gigatons of CO₂ through burning fossil fuels; this is often qualified as anthropogenic CO₂ emission [3]. Following that line of logic, humans have a large impact on the climate change crisis and often do not realize how large an effect it is having or could have on them. The current estimated cost of continuing to emit greenhouse gasses at the current rate to the U.S. is \$1.9 trillion annually due to hurricane damage, real estate loss, and energy and water costs attributed to climate change [4]. As the world continues to modernize and developing countries cross the threshold to being developed countries, energy needs and transportation needs will rise. If

nothing changes, greenhouse gas emissions will continue to increase. In 2018, energy production and transportation accounted for a combined 55% of greenhouse gas emissions in the United States [5]. If there were a way to use only electric vehicles and only renewable energy sources for power generation, it would be possible to strike a significant blow to anthropogenic CO₂ output and climate change.

Automotive industries are creating more efficient and enticing electric vehicles (EVs) and are slowly starting to promote and advertise them more. New, more complex, and faster-charging batteries and chargers are being created with new materials. Cutting edge research is being done on wireless energy transfer to personal EVs as they cross WPT coils powered by the energy grid integrated into the road near exits [6]. This increase in the sophistication of technology can create issues. One issue is that the new materials for EV batteries are often manufactured from rare earth elements like lithium. The extraction and production of increasingly complicated or an increased number of batteries would cause an increase in emissions and pollution [7]. The automotive industry's promotion of the use of PEVs would decrease overall emissions. Nevertheless, the EV's would still need to be charged using power. Currently, wired and wireless chargers for PEVs are connected to the power grid, and with an increase in EV use, power use would increase. This increase in power generation would increase emissions, which may be equivalent to the decrease in emissions from the replacement of internal combustion engine vehicles (ICEV's). This reliance on the grid reduces the overall effect technologies can have on climate change because power plants still rely heavily on fossil fuels.

Power companies are making progress, but in general, are not decreasing the use of fossil fuels for power generation [8]. However, power companies are decreasing coal and oil use for energy generation and increasing the amount of natural gas and renewable energy sources. This

move is an essential stopgap measure because burning natural gas for energy produces approximately 50% less CO₂ than coal and 20% less than oil and gas. There are two issues: one being the transition may not be fast enough, and the extraction methods such as fracking to retrieve the natural gas can be harmful to the environment [9].

A more broad and effective strategy must be devised to make the most significant possible impact. Each device or invention could be altered to increase the device's impact on decreasing greenhouse gas emissions, and if more companies worked together, this could be achieved more quickly. One idea is that if all the roads had wireless energy transfer systems, it could benefit PEV owners and the entire U.S. This WPT system would help increase the U.S. electric grid's efficiency, remove the need for overhead power lines, and increase EV range. It would also decrease the need for complex batteries, increase battery life, and reduce the issues of transportation emission of CO₂. It would also make EVs more accessible to the public as searching for a charging station or installing one in the owner's home would be unnecessary.

1.2 Background

Most researchers and companies interested in wireless power transfer focus on commercial items like phone chargers or chargers for medical devices. Wireless charging for these devices is meant to operate between 5mm-50mm and have an output power of 6.5W or below. Two groups are currently making WPT and WC standards, AirFuel Alliance (AFA) and the Wireless Power Consortium, and others are joining for different implementations. Most existing standards are for charging small devices. The current standards for small devices are Rezence, a resonantly coupled charging standard, and Qi and PMA, which are inductively coupled [10]. However, the

Society of Automotive Engineers (SAE) published a wireless charging standard for light-duty EV's and is working on one for heavy-duty EV's. SAE J2954™ is a standard supporting up to 11kW charging over a gap of 10 inches at 94% efficiency while the vehicle is stationary [11]. This standard could be beneficial for parking spaces, EV charging stations, and bus stops adding convenience to charging. These standards are all set at specific frequencies or frequency ranges and specify a power output. These standards have a few things in common. The objects, the charger and item being charged, must not be in motion relative to the other, must be within an acceptable range, and must be correctly oriented. Otherwise, charging is not initiated. This issue can be seen in current single-coil wireless chargers for phones. The phone will not charge unless it is at a specific point on the charger, and the coils are aligned over each. This limitation is often quite inconvenient for the end-user and lacks freedom. This thesis hopes to help overcome this limitation.

1.3 Thesis Objectives and Scope

As stated before, the current research, standards, and effort have been focused mostly on frequency-domain analysis of static systems, coil and circuit optimization, and system optimization and durability. This research will be talked about briefly in the next section. This thesis attempts to approximate a system for wireless charging of an in-motion device, specifically an EV, as a time-domain analysis. Currently, the Finite Element Method (FEM) is the gold standard for understanding complex systems over time. The issue with FEM is that it is resource-intensive, and accuracy is based on the resolution of the simulation run. FEM is beneficial for prototyping complex systems, but optimizing a system using FEM is often not

feasible within a reasonable time frame unless the company has many resources. Often researchers and industry must balance the cost in resources like time or computing power by reducing the resolution, thereby reducing the accuracy. This thesis attempts to create a model that can approximate a WPT system taking less time and resources to be used more easily for system optimization. More technologies and strategies can be applied to this model to make it easier for system optimization with given system parameters and constraints. These will be briefly talked about in later sections.

CHAPTER 2: LITERATURE REVIEW

2.1 Background

The overall principle that WPT works on is that an AC source going through a conductor causes the magnetic poles of the conductor to flip. When another conductor enters this magnetic field, the flipping magnetic poles or magnetic flux creates an electromotive force in the second. This phenomenon is known as Faraday's Law and causes current to flow through the second circuit, provided it has a load. This electromagnetic linkage in the conductors' fluctuating magnetic fields is called mutual inductance and has a strength associated with it. The mutual inductance between the two inductors can never be greater than the largest inductance of the inductors. In a perfect system, mutual inductance is calculated using the inductance values of the conductors with equation (1) below. The number more often referred to is the coupling coefficient and is the ratio of how strongly the conductors are coupled and has a maximum value of 100%. It is calculated using equation (2).

$$M = \sqrt{L_1 L_2} \quad (1)$$

$$k = \frac{M}{\sqrt{L_1 L_2}} \quad (2)$$

With the increased popularity of electric vehicles and the push by manufacturers like Tesla to make EV's cheaper and more accessible, methods to charge EVs are increasingly being researched. Currently, most of the focus is still on charging vehicles that are in place. Studies such as [12] look at the different forms of wireless power transfer, the impact of variables like coupling coefficient, frequency, quality factor, misalignment tolerance, and compensation

technologies. However, this is again where the wireless charging occurs in a static system. The Oak Ridge National Laboratory (ONRL) researchers talked about the benefits of in-motion WPT and tested a physical model in [13]. It addressed the effect of aluminum shielding, the effects of the road surface, and the efficiency, power output, and power factor at eight different configuration positions.

2.2 Coil Design and System Modeling Optimization

R. Tanzania et al. describes how the only losses in a WPT system come from parasitic impedances, and those losses increase with increased frequency [14]. This increase comes from the $j\omega$ term taken into account in AC circuits where $\omega = 2\pi f$ so the resultant inductive impedance increases linearly with frequency. [14] focuses on minimizing the AC resistance of a stationary WPT system, stress to the compensating capacitors, the power transfer efficiency, and using commercially available Litz wire to create the coils. R. Tanzia et al. concluded that a higher coupling factor and equal stress on the receiving and transmitting compensating capacitor minimizes the stress. It was also determined that a larger conduction area and higher frequency minimizes AC resistance. X. Lui et al. focused on optimizing spiral coil geometry and system parameters and built a physical model to test the relationships. The study found that tightly winding coils, the traditional method to maximize the coil's size, is not the most optimum geometry when considering efficiency and total power transfer. Most of the research on the optimization of the system is research into smart systems using power electronics or the use of IoT devices. J. Miller et al. explores the different ways to look at a stationary WPT system and having the primary side or the transmitting side be variable. It is suggested that if the primary

and secondary side processing units of the devices are in low latency communication that the variable primary side can modify its parameters such as frequency for optimal power transfer. C. Wang et al. researched using more than one resonant circuit and how to deal with bifurcation phenomena.

2.3 Issues

ONRL published [14] about what was learned during the testing and the challenges that need to be overcome to make In-Motion WPT a widespread reality. Some of the issues are common to both stationary and in-motion WPT. The similar issues are: power output vs. power necessary, secure low latency communication between the transmitting source and receiving device, loss of communication, more than one device is connected, scaling the system, and safety considerations. It also explores issues unique to in-motion dynamic systems such as synchronization, timing, and speed.

2.5 Benefits to Proposal

This thesis attempts to create a model to address the inconvenience of having to charge EV's while the vehicle is stationary. This thesis also looks to approximate the complex system of in-motion WPT and decrease the resource intensity and time it takes to run accurate simulations. The decrease in overall resource intensity would allow for implementing AI or machine learning techniques to optimize the system and coil parameters to get the most desirable system. The most desirable system could be different depending on the preferred outcome and constraints. These

constraints could be available space, the number of lanes, cost, required power or efficiency, or the need for consistent output power or voltage. Some significant benefits of implementing Wireless Power Charging (WPC) on the entire US road system are: batteries could be simplified, battery life would be increased, the range would be indefinite, cost of ownership would be far cheaper than current EV's and ICEV's, there would be little to no need to install chargers in the owner's house, and if adopted by all the CO₂ output from transportation by personal vehicles would be eradicated.

CHAPTER 3: METHODOLOGY AND DESIGN

3.1 Modeling the Coils and Circuit

Optimizing coil geometry is not the focus of this thesis, so geometry was decided using a few constraining factors. The coil's overall width was chosen to be 1.5m or approximately 5ft because the average width of road vehicles is 1.8m (6ft). This spacing leaves space allowing for easier access and maintenance to the coil and other existing parts. The wire chosen to create the coils is a 4-aught or 0000-gauge wire for safety due to the possibility of large current spikes.

Below is a representation of how a flat spiral coil is measured from [15].

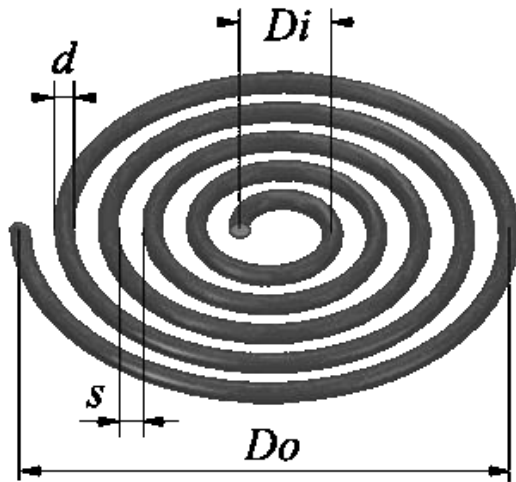


Fig. 1. Measurements for a Spiral Coil

The inner diameter (D_i) and winding pitch (s) are measured in the same fashion. The values are measured from center to center of the wires across the gap. The value for the coils used in this model is three times the wire diameter (d), making the gap equal to twice the wire diameter. This gap size is used to reduce the amount of parasitic capacitance between the windings. This model also assumes that the coil's parasitic capacitance is negligible. This assumption can be achieved using Litz wire, shielded wire, and increasing the winding pitch or reducing the number of turns in the coil. The inductance was attained using an online freeware calculator by Coil32 [15]. The previously stated parameters were entered into the calculator, and the "Required inductance" field was modified until the calculated coil diameter (D_o) was approximately 1.5m. The capacitance was calculated for both the receiving coil and the transmitting coil(s) to reach a specific resonant frequency derived from the resonance frequency formula below.

$$f_r = \frac{1}{2\pi\sqrt{LC}} \quad (3)$$

Solving (3) for capacitance at a specific resonant frequency and inductance results in the form below.

$$C = \frac{\left(\frac{1}{2f_r\pi}\right)^2}{L} \quad (4)$$

Wireless power transfer circuits can be modeled similarly to a coupled transformer or solenoid. A Series-Series Compensated topology for a resonant WPT system is the focus of this thesis and the simulations that were run. The transmitting side of the circuit is modeled as an AC source connected in series to a capacitor (C_p) and the primary or transmitting coil. The Receiving side of the circuit is similarly modeled but flipped. The receiving side is modeled as the

receiving coil in series with the secondary or receiving side capacitor (C_s) and the load resistance (R_L). The transmitting and receiving side are then joined parallel to each other by the mutual inductance of the coils (L_M). Each coil is represented as the coil's resistance (R_p or R_s) and inductance (L_p or L_s). The resistor is the coil's resistance, which is calculated by multiplying the length of wire required to make the coil times the resistance per meter resulting in a value in Ohms. The inductance value of each inductor is time-dependent in this system because it varies with mutual inductance. Mutual inductance changes depending on the receiving coil's relative position to the transmitting coil(s). As such, the inductance values are quantified as $L_p - L_M$ for the transmitting coil, $L_s - L_M$ for the receiving coil, and L_M for mutual inductance. This process is shown by the circuit diagram below and corroborated by [12], [16], [6].

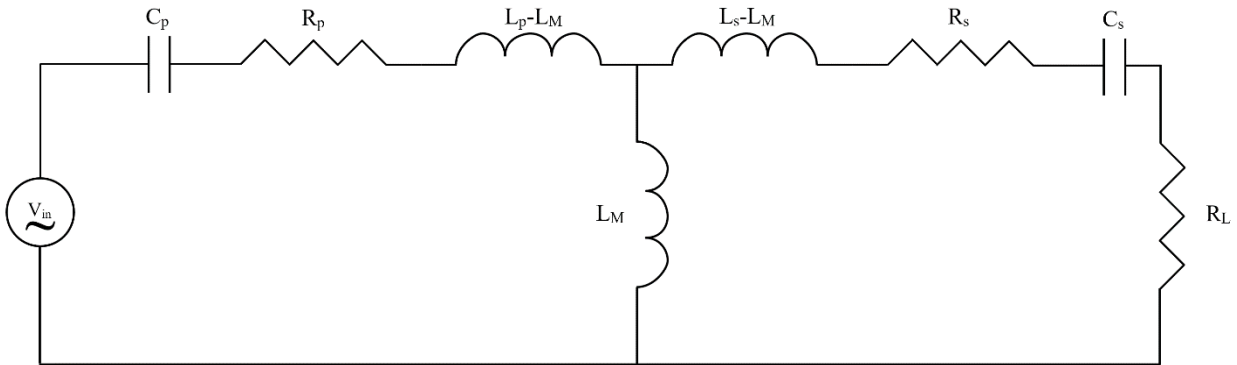


Fig. 2. Series-Series Compensated WPT Circuit

Once the circuit was established, the next step is to solve it. An equivalent circuit was created using Thevenin's Theorem and then solved to get the load resistor's output voltage. To calculate the Thevenin impedance, the voltage source was shorted, and the load resistance was removed. The components were then converted into impedances and grouped as blocks resulting in the circuit on the left below. The Thevenin source and Thevenin impedance were calculated, and then the load impedance was replaced, resulting in the Thevenin equivalent circuit below on the right.

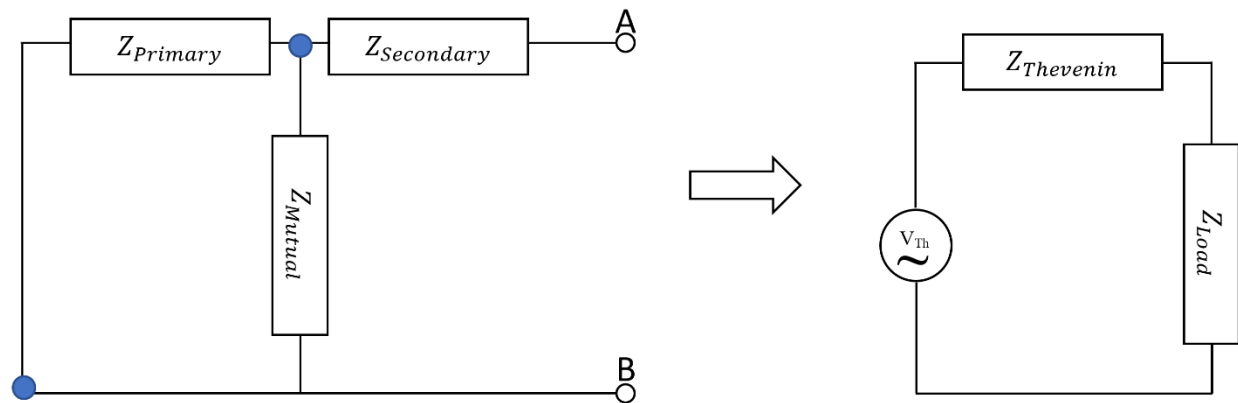


Fig. 3. Reduction of WPT Circuit Using a Thevenin Equivalent Circuit

In fig. 3., the Z_{Primary} consists of the coil, which is made of the resistor and inductor (R_p and $L_p - L_M$), and the compensating capacitor of the transmitting side (C_p). $Z_{\text{Secondary}}$ consists of the coil, which is made of the resistor and inductor (R_s and $L_s - L_M$), and the compensating capacitor of the receiving side (C_s). Z_{Mutual} is the mutual inductance. Z_{Load} is the resistive load (R_L). Z_{Primary} and Z_{Mutual} are in parallel with each other and series with $Z_{\text{Secondary}}$ resulting in the equations for Z_{Thevenin} , Z_{Total} , V_{Th} , and V_{Out} below:

$$Z_{\text{Thevenin}} = Z_{\text{Secondary}} + Z_{\text{Primary}} \parallel Z_{\text{Mutual}} = Z_{\text{Secondary}} + \frac{Z_{\text{Primary}} \times Z_{\text{Mutual}}}{Z_{\text{Primary}} + Z_{\text{Mutual}}} \quad (5)$$

$$Z_{\text{Total}} = Z_{\text{Load}} + Z_{\text{Thevenin}} = Z_{\text{Load}} + Z_{\text{Secondary}} + \frac{Z_{\text{Primary}} \times Z_{\text{Mutual}}}{Z_{\text{Primary}} + Z_{\text{Mutual}}} \quad (6)$$

$$V_{\text{Thevenin}} = V_{\text{in}} \times \frac{Z_{\text{Mutual}}}{Z_{\text{Primary}} + Z_{\text{Mutual}}} \quad (7)$$

$$V_{\text{out}} = V_{\text{Thevenin}} \times \frac{Z_{\text{Load}}}{Z_{\text{Load}} + Z_{\text{Thevenin}}} \quad (8)$$

Now V_{Thevenin} is substituted into V_{out} , resulting in the equations below:

$$V_{\text{out}} = V_{\text{in}} \times \frac{Z_{\text{Mutual}}}{Z_{\text{Primary}} + Z_{\text{Mutual}}} \times \frac{Z_{\text{Load}}}{Z_{\text{Load}} + Z_{\text{Secondary}} + \frac{Z_{\text{Primary}} \times Z_{\text{Mutual}}}{Z_{\text{Primary}} + Z_{\text{Mutual}}}} \rightarrow \quad (9)$$

$$V_{\text{out}} = V_{\text{in}} \times \frac{Z_{\text{Load}} \times Z_{\text{Mutual}}}{Z_{\text{Load}}(Z_{\text{Primary}} + Z_{\text{Mutual}}) + Z_{\text{Secondary}}(Z_{\text{Primary}} + Z_{\text{Mutual}}) + Z_{\text{Primary}} \times Z_{\text{Mutual}}} \quad (10)$$

This equation can now be rearranged and modified to make the multiplication and term simplification easier. Z_{Primary} and $Z_{\text{Secondary}}$ are made from three different components. As such, minimizing the number of times these are multiplied by will make the simplification easier. The equation below is equivalent but reduces multiplication by Z_{Primary} and $Z_{\text{Secondary}}$.

$$V_{\text{out}} = V_{\text{in}} \times \frac{Z_{\text{Mutual}} \times Z_{\text{Load}}}{Z_{\text{Primary}} \times Z_{\text{Secondary}} + Z_{\text{Mutual}}(Z_{\text{Primary}} + Z_{\text{Secondary}}) + Z_{\text{Load}}(Z_{\text{Primary}} + Z_{\text{Mutual}})} \quad (11)$$

Now that the circuit is effectively solved, the bundled inductances now need to be replaced by their component values.

$$V_{out} = V_{in} \times \frac{sR_L L_M}{\left(R_p + s(L_p - L_M) + \frac{1}{sC_p}\right)\left(R_s + s(L_s - L_M) + \frac{1}{sC_s}\right) + sL_M \left(R_p + s(L_p - L_M) + \frac{1}{sC_p} + R_s + s(L_s - L_M) + \frac{1}{sC_s}\right) + R_L \left(R_p + s(L_p - L_M) + \frac{1}{sC_p} + sL_M\right)} \quad (12)$$

Once the terms are fully multiplied, reduced, and grouped by the terms power, the equation is as follows:

$$V_{out} = V_{in} \times \frac{sR_L L_M}{s^2(L_p L_s - L_M^2) + s^1(R_p L_s + R_s L_p + R_L L_p) + s^0(R_p R_s + R_p R_L + \frac{L_p}{C_s} + \frac{L_s}{C_p}) + s^{-1}(\frac{R_p}{C_s} + \frac{R_s}{C_p} + \frac{R_L}{C_p}) + s^{-2}(\frac{1}{C_p C_s})} \quad (13)$$

This formula can now be used to calculate the output voltage at any specific moment in time. To use this equation for time-domain analysis, it needs to be used repeatedly, and the variable values such as L_M and V_{in} need to be updated each time the equation is used. This system can be modeled in phase variable canonical form using Mason's Gain Formula [16], which is shown below.

$$G(s) = \frac{\sum_k P_k}{1 - \sum_{q=1}^N L_q} = \frac{\text{Sum of the forward-path factors}}{1 - \text{sum of the feedback loop factors}} \quad (14)$$

To get the equation into the proper form, multiply the numerator and denominator by s^2 , so the denominator has a minimum power of s^0 . If the coils are the same, the formula can be simplified further, resulting in equation (16). R is the coil's resistance, L the coil's inductance, C the compensating Capacitance, R_L the load resistance, and L_M the mutual inductance.

$$V_{out} = V_{in} \times \frac{s^3 R_L L_M}{s^4(L_p L_s - L_M^2) + s^3(R_p L_s + R_s L_p + R_L L_p) + s^2(R_p R_s + R_p R_L + \frac{L_p}{C_s} + \frac{L_s}{C_p}) + s^1(\frac{R_p}{C_s} + \frac{R_s}{C_p} + \frac{R_L}{C_p}) + s^0(\frac{1}{C_p C_s})} \quad (15)$$

$$V_{out} = V_{in} \times \frac{s^3 R_L L_M}{s^4(L^2 - L_M^2) + s^3(2LR + LR_L) + s^2(RR_L + \frac{2L}{C} + R^2) + s^1(\frac{2R + RL}{C}) + s^0(\frac{1}{C^2})} \quad (16)$$

To modify the equation into the final form of one minus the rest of the terms in the denominator, the numerator and denominator must be divided by the s^4 phase variable. This division will be implemented in the simulation to simplify solving the equation further. As such, the next step is to model mutual inductance.

3.2 Modeling Mutual Inductance

Mutual inductance depends on the receiving coil's position relative to the transmitting coil, the coils' geometry, and the medium through which the coils are trying to inductively couple. To simplify the model and testing, the coils were made to be parallel to each other at all times. During the simulations, the Y and Z offset are held constant as the receiving coil moves in the X-direction. The equation used to calculate mutual inductance is based on the equations in [17]. As stated before, the coils are parallel at all times, so the tilt angle, represented by theta in the equation, is zero. The initial equation modified to have a non-zero center point for the transmitting coil is below.

$$M = \frac{\mu_0}{4\pi} a_1 a_2 \int_{\phi_{i_2}}^{\phi_{o_2}} \int_{\phi_{i_1}}^{\phi_{o_1}} \frac{\cos \theta (\cos \varphi_1 - \varphi_1 \sin \varphi_1) (\cos \varphi_2 - \varphi_2 \sin \varphi_2) + (\sin \varphi_1 + \varphi_1 \cos \varphi_1) (\sin \varphi_2 + \varphi_2 \cos \varphi_2)}{\sqrt{((X_2 + a_2 \varphi_2 \cos \varphi_2 \cos \theta) - (X_1 + a_1 \varphi_1 \cos \varphi_1))^2 + ((Y_2 + a_2 \varphi_2 \sin \varphi_2) - (Y_1 + a_1 \varphi_1 \sin \varphi_1))^2 + (Z_2)^2}} d\varphi_1 d\varphi_2 \quad (17)$$

Figure 3 in that same paper shows that $d \cos(\alpha)$ represents the distance in the X direction between the centers of the receiving and transmitting coil as it is projected on the plane of the transmitting coil. Distance in the Y direction in the equation is represented as $d \sin(\alpha)$. Using that and the information given immediately after equation 12, the equation can be modified to be used for time-domain modeling. The changes made to the equation to use it with a rectangular coordinate system and holding the coils parallel is that the numerator is simplified

and equivalent to the numerator of equation 10 when $\theta = 0$. The next change is that the denominator of equation 12 is used, but (X_0, Y_0, Z_0) are replaced with the (X, Y, Z) position of the secondary coil and the (X, Y, Z) position of a non-zero center of the transmitting coil is added to each term in the denominator. The denominator, which is the 3D-space distance formula, is then in the form $\sqrt{(X_2 - X_1)^2 + (Y_2 - Y_1)^2 + (Z_2 - Z_1)^2}$. A subscript was added to the (X, Y, Z) coordinates of the transmitting coil to denote which transmitting coil and corresponding (X, Y, Z) values should be used, allowing for multiple transmitting coils. The Z value of the transmitting coils is always zero and because the value of $\sin(0) = 0$ the Z term in the denominator is simply Z_s^2 . These changes result in the equation below.

$$M = \frac{\mu_0}{4\pi} a_1 a_2 \int_{\phi_{i_2}}^{\phi_{o_2}} \int_{\phi_{i_1}}^{\phi_{o_1}} \frac{(1+\varphi_1\varphi_2)+\cos(\varphi_2-\varphi_1)-(\varphi_2-\varphi_1)(\sin(\varphi_2-\varphi_1))}{\sqrt{((x_s+a_2\varphi_2 \cos \varphi_2)-(x_{p(i)}+a_1\varphi_1 \cos \varphi_1))^2 + ((y_s+a_2\varphi_2 \sin \varphi_2)-(y_{p(i)}+a_1\varphi_1 \sin \varphi_1))^2 + (z_s)^2}} d\varphi_1 d\varphi_2 \quad (18)$$

The equation, code, and simulation could be edited to allow for paths that are not straight in 3D space, variable velocity, height, roll, and coil pitch. The coil's yaw or spin has a negligible effect on the mutual inductance due to spiral coils' symmetry. This fact was proven in [17] and tested and verified in the model proposed in this thesis before use.

3.3 Modeling the System in Simulink® and MATLAB®

The script in Appendix A was written to allow quick modification of system and coil parameters and calculate the Mutual inductance over time. The first half contains the coil parameters needed for the equations in [17] and the frequency, velocity, V_{in} , R_L , height (Z_s), PPC, NumCoil, and spacing. PPC is points per coil, which refers to how many data points are being calculated for each transmitting coil's mutual inductance curve. NumCoil is the number of

transmitting coils. Spacing is a variable used to set the distance between the transmitting coils. PR is a calculated value obtained by dividing the outer diameter of the transmitting coil by PPC to give how frequently in meters a data point is taken. TD is the total distance traveled in the simulation, calculated using one of the three formulas below, depending on the transmitting coils' layout. The center of the receiving coil always starts on the origin. However, the total distance depends on how the transmitting coils are set up. The set-ups that were modeled in this thesis are if the graph starts with the transmitting coil first, spacing first, or half spacing first. A graphical representation of having the transmitting coil first and having half-spacing first is drawn below. The spacing distance is S, and the diameter of the transmitting coil is TCD.



Fig. 4. Graphical Representation of the Equivalency of the Coil Spacing

Adding together the distance covered of these two cases shows that an equivalent distance is traveled with these two methods, as shown by the equation below.

$$\frac{1}{2}S + \frac{1}{2}S + S + TCD + TCD = TCD + TCD + S + S \quad (19)$$

The next case is if a full space is placed first and is represented below.

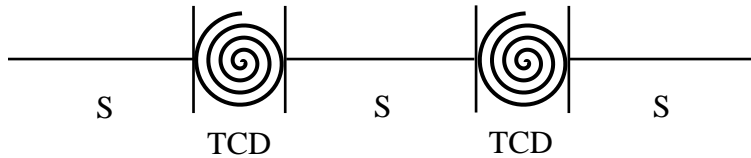


Fig. 5. Graphical Representation of Full Spacing

The total distance traveled, in this case, is represented by the equation below.

$$TD = TCT + TCD + S + S + S \quad (20)$$

These equations can then be modified into the equations below to calculate the total distance traveled, depending on the number of transmitting coils.

$$\text{Coil First or Half-spacing First: } TD = Spacing * NumCoil + NumCoil * (OR_P * 2) \quad (21)$$

$$\text{Spacing First: } TD = Spacing * (NumCoil + 1) + NumCoil * (OR_P * 2) \quad (22)$$

The total distance is the same, whether the coil or a half-space is placed first. This equality occurs because the spacing is placed after the second transmitting coil when starting with the transmitting coil first. Resolution is calculated as TD/PR, and t_end is how long in seconds it takes to cross the total distance and is calculated by TD/velocity. The second half of the file sets the receiving coil's movement and the transmitting coils' position, which depends on

the spacing format used above. The equations below calculate where the centers of the transmitting coils are. Where $x_{p(1,i)}$ is the x-coordinate for the center of the i^{th} transmitting coil to allow larger models to be run.

$$\text{Transmitting Coil First: } x_{p(1,i)} = ((2 * i - 1) * OR_p) + ((i - 1) * Spacing) \quad (23)$$

$$\text{Spacing First: } x_{p(1,i)} = ((2 * i - 1) * OR_p) + i * Spacing \quad (24)$$

$$\text{Half-spacing First: } x_{p(1,i)} = ((2 * i - 1) * OR_p) + ((i - 0.5) * Spacing) \quad (25)$$

The Y and Z values for the transmitting coil's centers are set to zero as the transmitting coils are all static and the reference point for the receiving coil that is in motion. The mutual inductance over time is then calculated and plotted to show the mutual inductance over time, which generally looks like a bell curve with the highest mutual inductance value occurring when the center of the transmitting coil is directly over the center of the receiving coil. An example of a mutual inductance curve is shown below. The black dashes represent the edges of the transmitting coils, and the red dash represents the center of the transmitting coils.

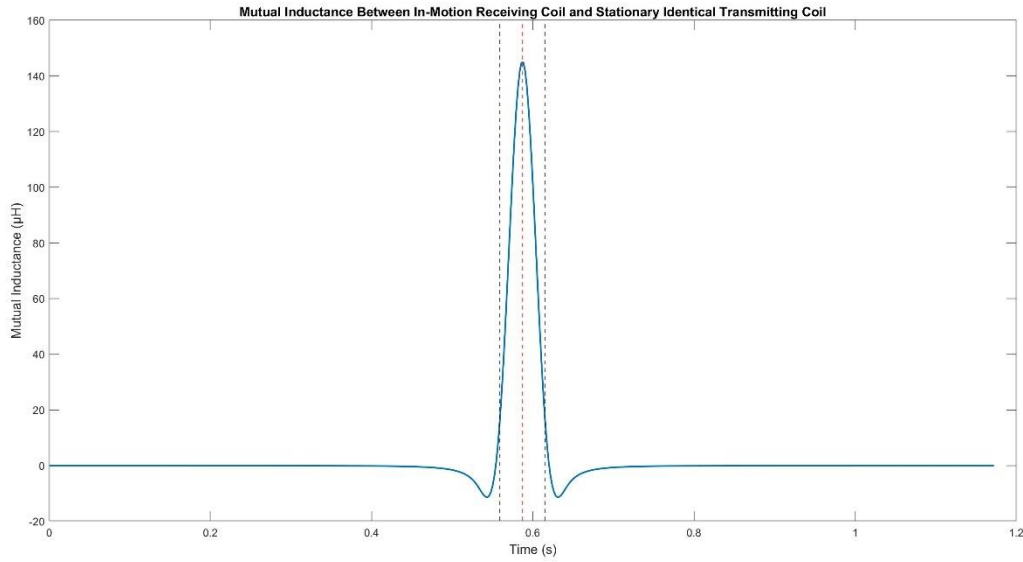


Fig. 6. Mutual Inductance for Identical Coils Using Default Parameters

The Simulink® model calculates the output voltage (V_{Out}) across the load resistor and sends it to the MATLAB® workspace as a time-series. The time-series gives the V_{Out} value at every time (t) that was solved. The model also solves for the output power by using the calculated V_{Out} and Ohm's law $P = \frac{V^2}{R}$. The Simulink® simulation uses the ODE4 Runga-Kutta fixed-step solver starting at a time of zero and ending at t_{end} . The step size is based on the PPC following the Nyquist-Shannon sampling theorem the sample size of the fixed-step solver must be at least twice the PPC. Therefore, the equation for the fixed step size is below:

$$\text{Fundamental Sample Time or Fixed Step Size: Step size} = \frac{1}{f \times 50} \quad (26)$$

The periodic sample time is unconstrained. Now the data must be run in the Simulink® model. The model is pictured below.

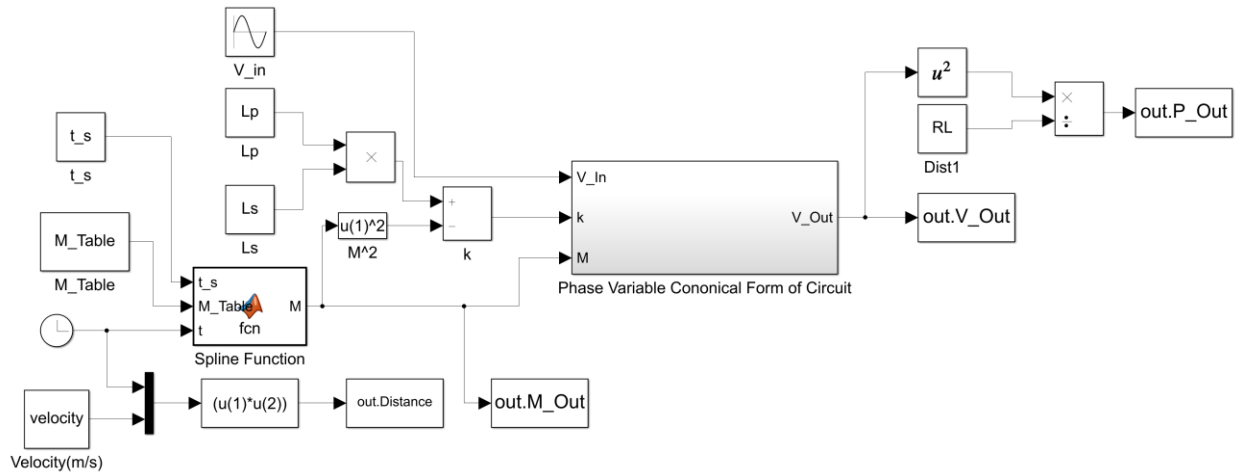


Fig. 7. Block Diagram of the System Modeled in Simulink®

This simulation takes the calculated mutual inductance values (M_Table) and inputs them into the built-in MATLAB® spline function. The spline function allows the mutual inductance to be interpolated at any point in time. The spline uses the calculation of velocity multiplied by time to see where the center of the receiving coil is at that point in time and feeds that position into the spline as a query point. V_{in} is the input voltage, which for all tests in this proposed model is a

120V AC wave at a specified frequency. The value of k in the simulation is equal to the s^4 phase variable in (15), which all states must be divided by to format the equation to match Mason's Gain Formula properly. The state-space model is shown below.

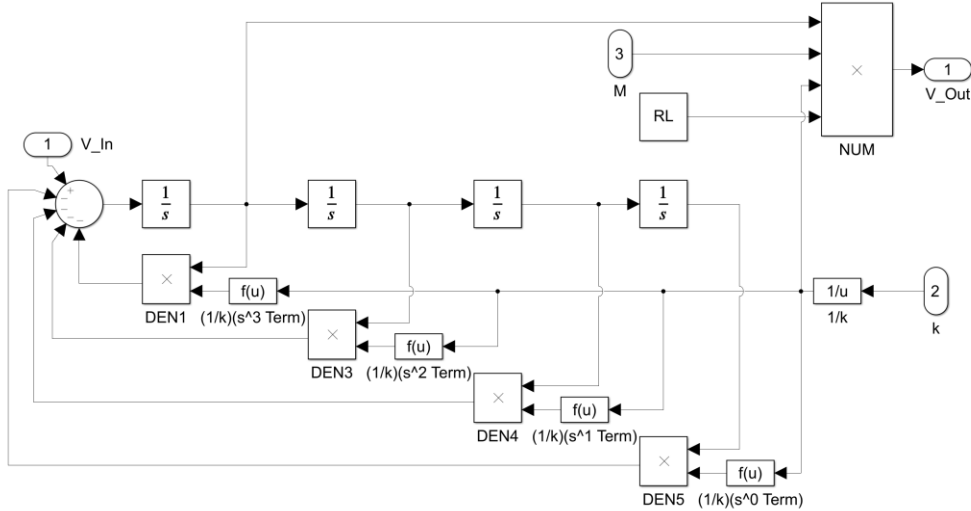


Fig. 8. Phase Variable Canonical Form Simulation Block Internal

The left-most integrator, represented by the $\frac{1}{s}$ block is the s^4 phase variable, and each integrator after that block is one power of s less. The feedback loop factors represented by the DEN blocks are a multiplication of each term by the integrator of that term, and each loops back to be subtracted from V_{in} . The forward factors in Mason's Gain Formula are the terms in the

numerator of (15). The forward factors are represented in the top right where the load resistance, mutual inductance, and s^3 phase variable are multiplied and then divided by k resulting in V_{out} . V_{out} is then squared element-wise and divided by R_L to get P_{Out} . To determine the Simulink® simulation was outputting the correct values, the transfer function (15) was solved at multiple points in time and compared to the simulation's output at the same points in time. The results matched, and the model was determined to be working correctly.

3.4 Modeling a System with Multiple Transfer Coils

To modify this model to use multiple transmitting coils, a few changes must be made, and the coils must be spaced far enough apart so that coupling between the transmitting coils does not occur at any point in time. Shown below is an example showing that if the coils are spaced far enough apart. The waveform repeats, and the values between the waveforms are at or near zero.

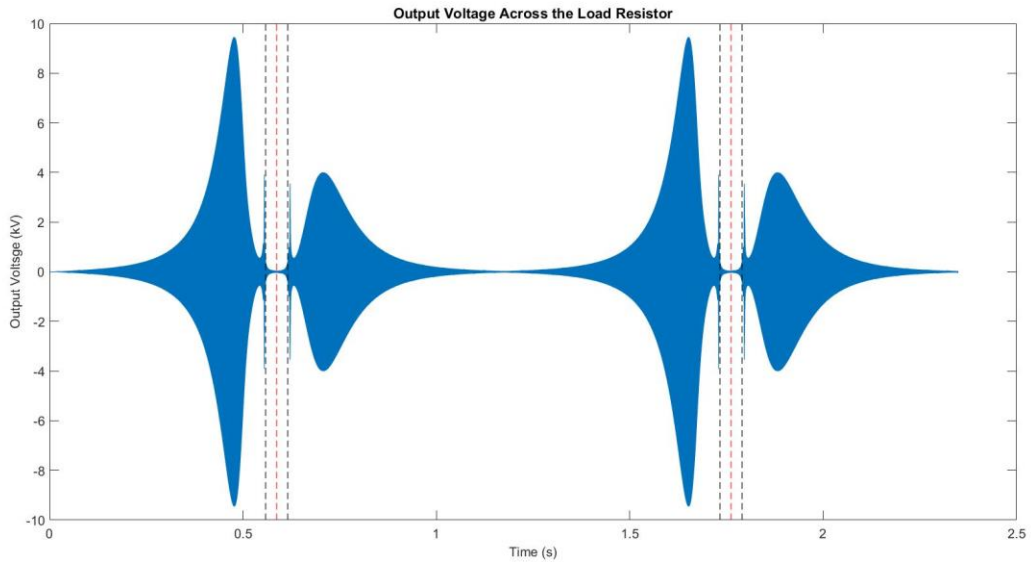


Fig. 9. Output Voltage of a Two Transmitter Coil System with Identical Coils

The variable NumCoil needs to be changed to the number of transmitting coils desired. The mutual inductance calculation's for loop should be duplicated, the data points distributed evenly between the coils in the for loop's conditions, and the indices modified to fit the changes. If the coils are not properly spaced, the mutual inductance equation becomes much more complicated. The mutual inductance between the receiving coil and each transmitting coil and between each transmitting coil that is linked to another transmitting coil would have to be calculated and accounted for by modifying the circuit diagram. This complex situation is outside the scope of the proposed model.

3.5 Model Modification for Understanding Effects of Variables on the System

The model was run many times using different values for one variable at a time to discern the effects of each variable on the shape of the waveform and total output power. As stated before, most current studies have been done on stationary coils directly over each other. These studies show that coil geometry, frequency, and the vertical, horizontal, and angular offset of the receiving coil are significant factors in the efficiency and total power transferred. More variables can be inspected due to the dynamic nature of the system. It was decided that five trials would be run for five variables to see the isolated effect of each on the waveform and energy output. The variables tested were frequency, load resistance, X- alignment, Y-alignment, the height of the receiving coil (Z-offset), the receiving coil's speed, and the effect of using a half-sized receiving coil. The effect of the receiving and transmitting coils being different in size was also tested with the five variables.

The frequency values were chosen by setting the desired resonant frequency as the middle and values 100kHz above and below were chosen until there were five values in total. The speed values are typical U.S. speed limits in miles per hour, 20, 35, 45, 60, and 70, converted to meters per second. The Y-offset starts at zero and increases by the transmitting coil's radius and is then doubled until five values are obtained. The Z-offset starts at the average clearance height in meters of personal vehicles 0.1178m (7in), increases to the radius of the transmitting coil, and then was doubled until there were five values. The load resistances were re-worked during simulation because some values caused the simulation to diverge and fail. The final load resistances chosen were chosen because they are common products and readily available, 100Ω 10Ω , 1Ω , 0.1Ω , and 0.01Ω . The default case is when the frequency is

300kHz, R_L is 100, velocity is 26.8224 m/s, Z-offset is 0.1778m, and Y-offset is 0m. Only one variable value is changed per run, and all other values are set to the default case values.

In most cases, the code and simulation were run after changing a single variable value to see the effect of that change, and then the next value was tested. However, the way the code is set up makes it possible to reduce the number of times the mutual inductance code was run. If only changing the load resistance or the frequency, it is unnecessary to run the mutual inductance curve calculations for each change as they are not used in the calculation. Before running the simulation, if changed, the load resistance would need to be updated and or the frequency and ω must be updated. These variables are represented by the variable name used in the Simulink® model. The Simulink® model reads the current values of those variables before running and then runs the simulation. Once the simulation was finished, a graph of V_Out was saved, and the overall energy output was calculated using the built-in MATLAB® function trapz. Trapz can be used to take the integral of a variable with respect to another. The result of the function is the energy output in terms of Watt seconds. These values and effects of variables on waveforms are compared below.

CHAPTER 4: RESULTS

4.1 General Testing Results

As stated previously, in all the following results, the system's parameters were all default, except a single variable value was modified. The line graphs represent the resultant overall power transferred for the different values of each variable. The figure below shows the effect of load resistance on the system's output power for identical coils at default conditions and two different resistances. The default condition is 100Ω ; as the resistance decreases, the waveform seems to stretch as if pulled from the left and the right. The magnitude of the spikes decreases, and the average power transferred is higher with the 0.1Ω resistance. The increased power transfer is due to an increased amount of time where the energy is gathered and increased values in areas other than the spikes.

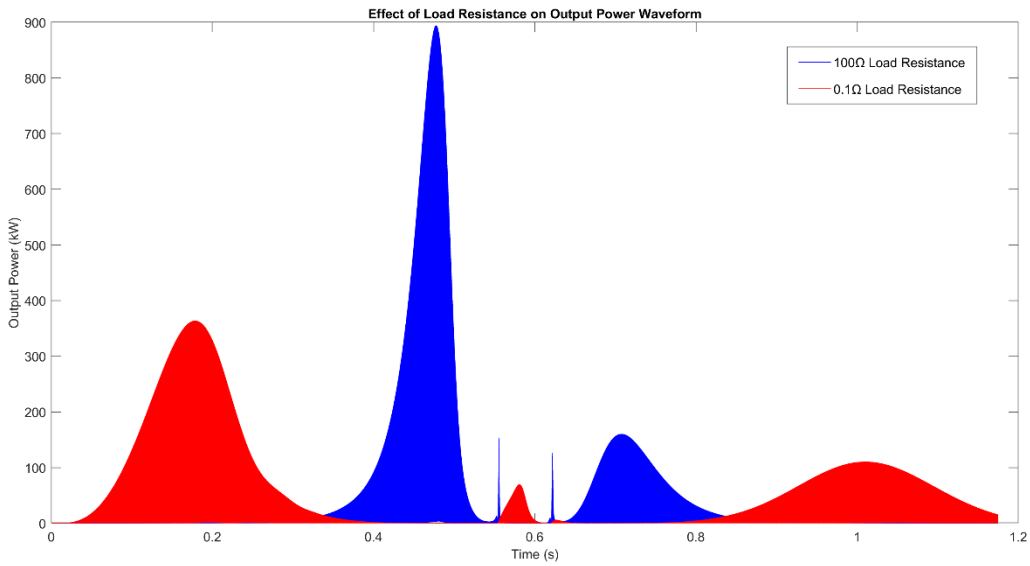


Fig. 10 Effect of Load Resistance on the Output Voltage Waveform of Identical Coils

4.2 Identical Transmitting and Receiving coil

The first variable changed to discern the effect was frequency. The system was designed for a specific resonant frequency, so it was understood that there would be little to no power transfer at values far from the resonance frequency. The results are shown below.

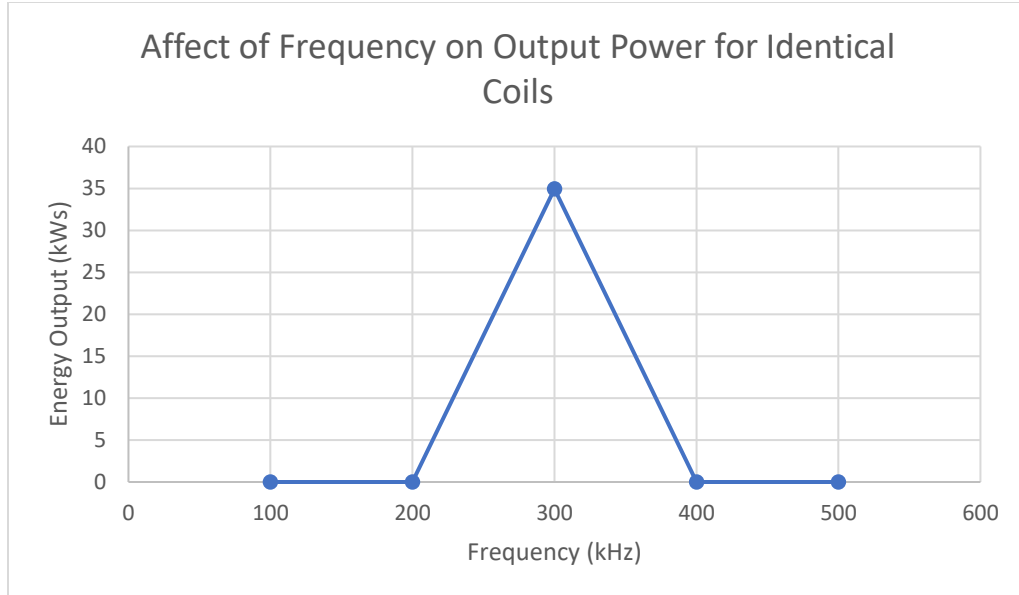


Fig. 11. Affect of Frequency on Output Power for Identical Coils

The next variable to be changed was speed. Intuitively the slower the vehicle moves over the same distance, the longer it will take to reach the end. This increased time allows for more time for power to be transferred and more cycles to occur. The trend line looks like a power regression, and the results are shown below.

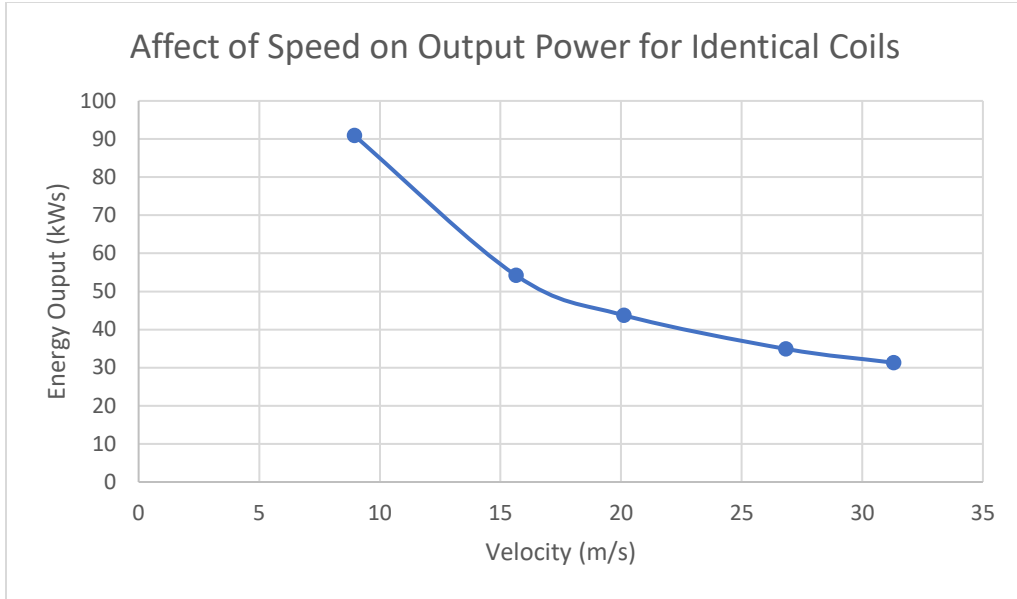


Fig. 12. Affect of Speed on Output Power for Identical Coils

For all systems, a set of optimal parameters exists. When talking about power transfer, most will refer to the maximum power transfer theorem, which states that maximum power occurs at 50% efficiency. The results of modifying the load resistance are shown below.

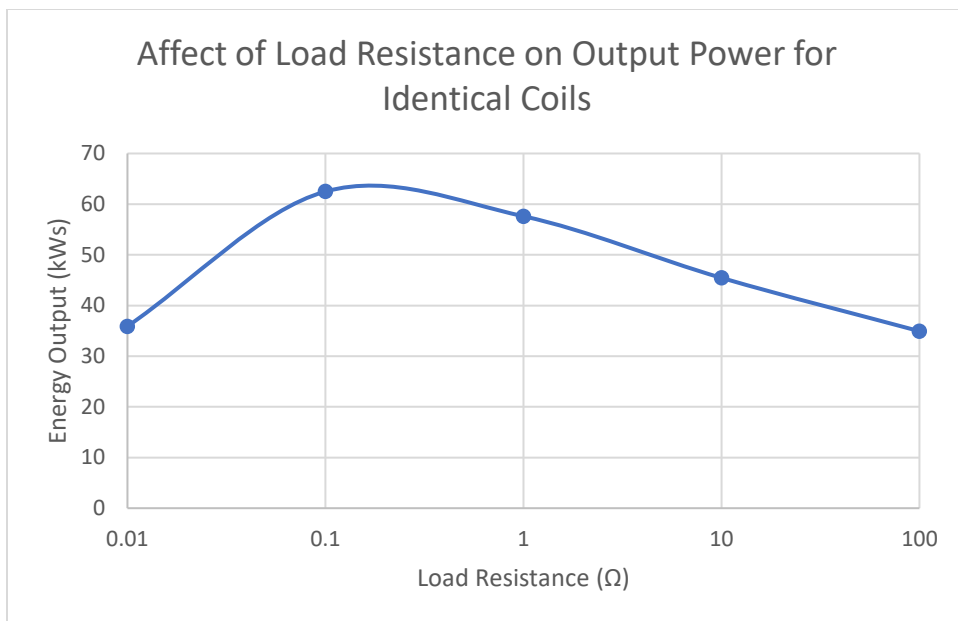


Fig. 13. Affect of Load Resistance on Output Power for Identical Coils

The lateral misalignment or Y-Offset is a measure of how far to one side the receiving coil is while it travels along the straight path across the transmitting coil. If more data points were taken, there would be a point where the trendline in the graph below would drop towards no power transfer as the coils would be too far to couple.

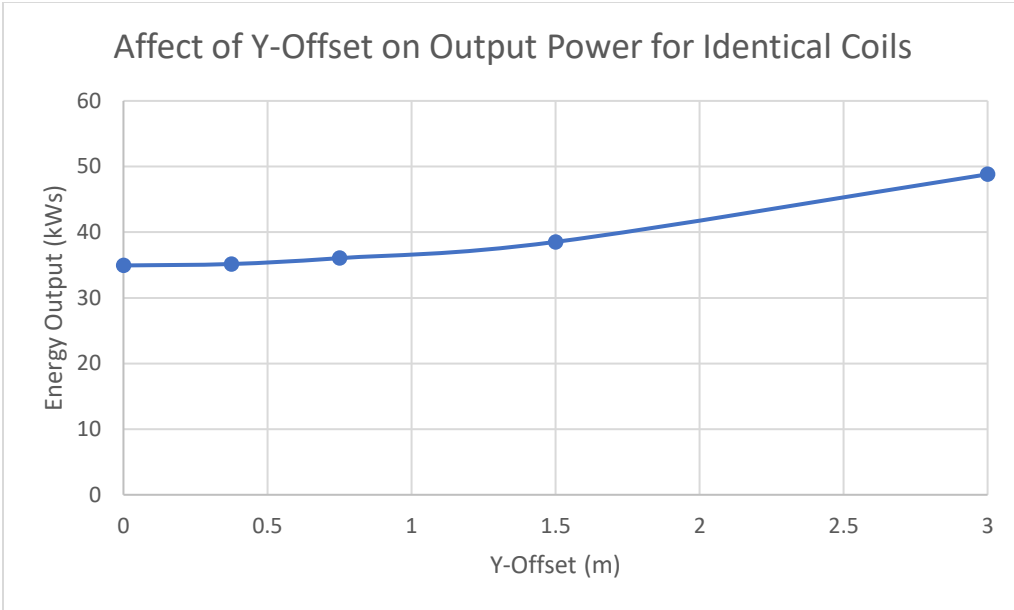


Fig. 14. Affect of Y-Offset on Output Power for Identical Coils

In general, for WPT systems, the vertical distance between the transmitting and receiving coil or Z-offset is a significant factor that affects the power transfer and efficiency. The graph below shows the results of the simulations run.

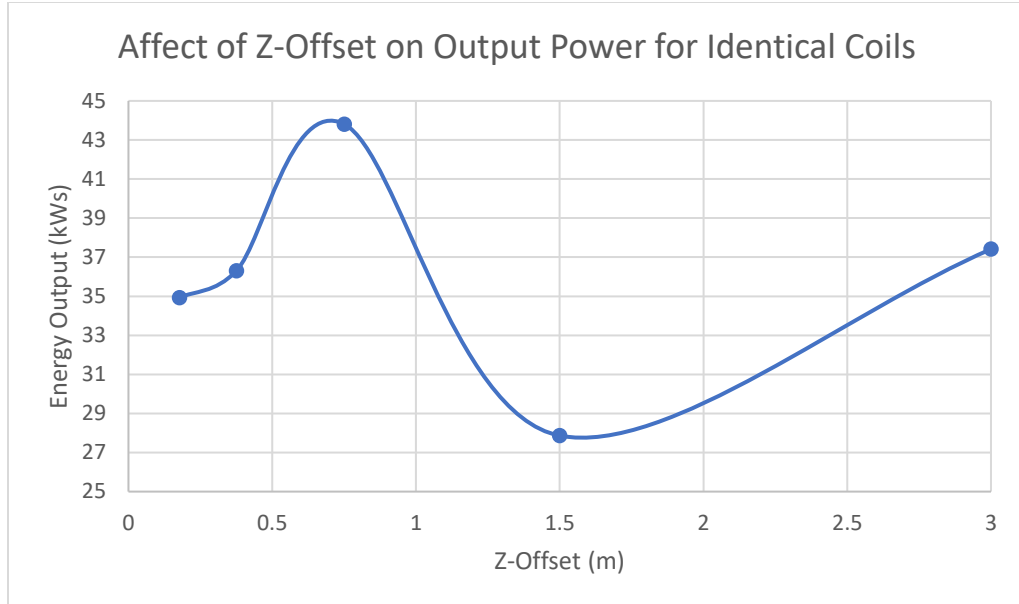


Fig. 15. Affect of Z-Offset on Output Power for Identical Coils

4.3 Non-Identical Transmitting and Receiving coil

The results for the half-size coil all had some similar effects but others that were not. The effect of frequency, in this case, was the same.

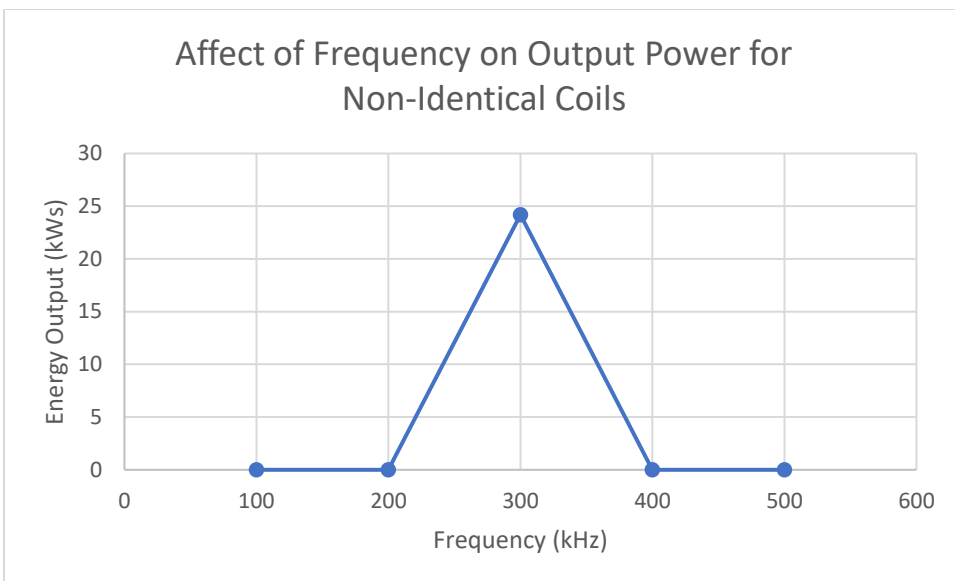


Fig. 16. Affect of Frequency on Output Power for Non-Identical Coils

The effect of speed on the total amount of power also follows a similar trend as the identical coils. The main difference is that less power is transferred. A little more than half as much was transferred.

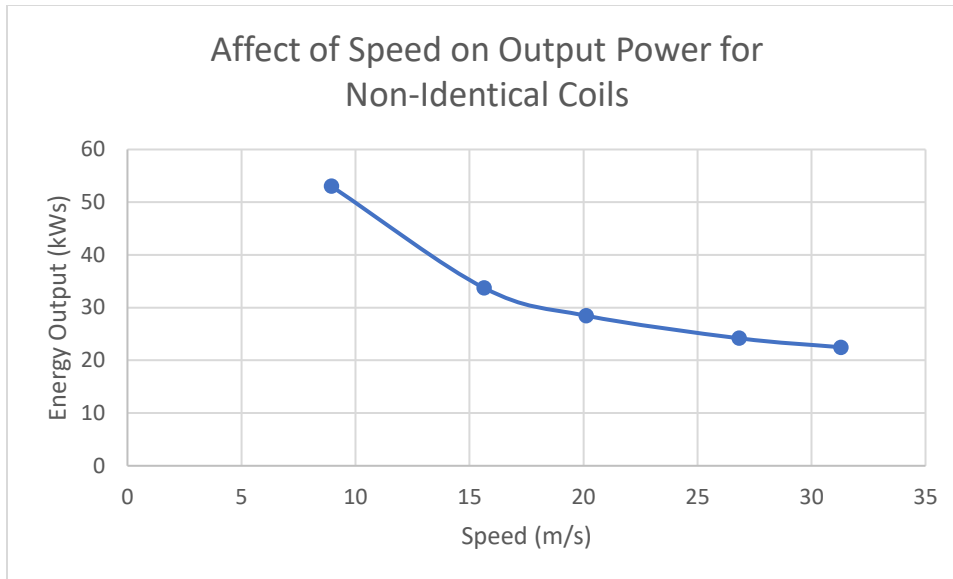


Fig. 17. Affect of Speed on Output Power for Non-Identical Coils

However, the trendline of the effect of load resistance on output power followed a different pattern than the identical coils. The effect of load resistance on the identical coils was almost like a bell curve, where power output gradually decreases to the left and right of a maximum point. The effect of load resistance on non-identical coils is different. The trendline to the left of 0.1Ω seems as though it is beginning to level off, whereas to the right, the output power is dropping rapidly. As such, decreasing the resistance below 0.1Ω seems to have negligible effects on this system. More data points and resolution would be needed to confirm this.

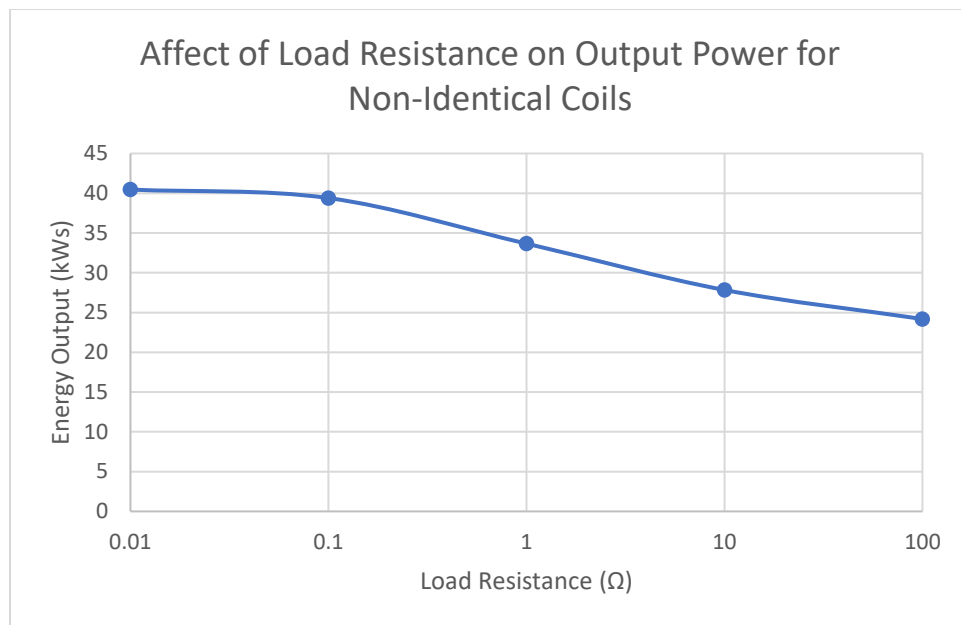


Fig. 18. Affect of Load Resistance on Output Power for Non-Identical Coils

Changing Y-Offset was another trend that differed for identical and non-identical coils.

For identical coils, the trend line was like a slowly increasing power curve. For the non-identical coils, the trendline seems to have a range of effective power transfer with an optimal point for maximum power transfer, whereafter the power transferred begins to drop sharply.

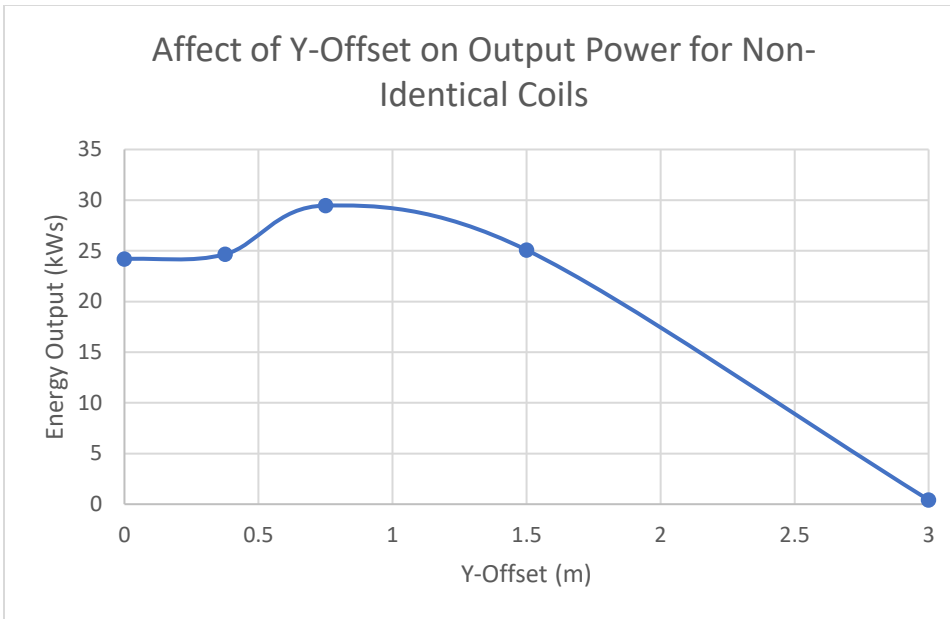


Fig. 19. Affect of Y-Offset on Output Power for Non-Identical Coils

Modifying the Z-Offset seems to have a bifurcation event. There are two similar peak areas with local maxima with steep drops to each side and a slight drop between the two local maxima.

Affect of Z-Offset on Output Power for Non-
Identical Coils

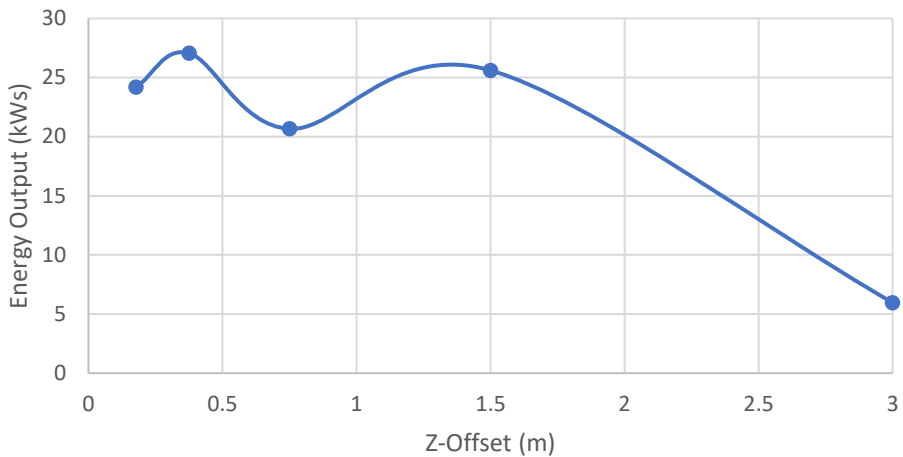


Fig. 20. Affect of Z-Offset on Output Power for Non-Identical Coils

CHAPTER 5: CONCLUSION AND FUTURE WORK

5.1 Conclusion

This model accurately calculates the mutual inductance of a receiving coil in-motion over a transmitting coil(s) and the resultant voltage and power output across the load resistor on the receiving coil when the constraints mentioned previously are observed. The constraints being that the transmitting coils must be spaced such that at all points in time, no coil has mutual inductance with more than one other coil. Running the mutual inductance script on a modern laptop (8 core, 16 thread, at average 4.6GHz and 70% usage) took, on average, twenty minutes per run. Running the Simulink® simulation took, on average, an hour per run. In [17], the FEM simulations in ANSYS Maxwell took over ten hours to model the mutual inductance between a stationary transmitting and receiving coil. This model will likely show a considerable improvement in resource intensity and the amount of time it takes to approximate the WPT of an in-motion receiving coil. As shown in the results, some combinations of variables can create unrealistic systems to implement in the real world. Looking at the results, the most power transferred occurred at the resonant frequency. With more data points and a finer resolution centered around the resonant frequency, there could be a tolerance or range where the frequency may not be precisely 300kHz but would still transmit more than 90% of the power transferred at the resonance frequency. There are an optimal set of parameters in each case, but combining all of the optimal cases for each variable and using the values together may not give the most optimal or maximum power transfer of the system. The equation is complex and time-variant, so trying to optimize the system would require analyzing trends and or using machine learning and

AI to brute force calculate the optimum.

5.2 Future Work and Considerations

If the input energy or power were calculated, it would be possible to calculate the system's efficiency, explore the maximum power transfer (MPT), and find a balance between efficiency and the MPT. This model could be compared to a FEM analysis to determine how accurate the results are and compare the resource intensity and required time. This comparison would help prove that this model could be used for rapid prototyping, and then FEM could be used when optimal cases are found. Machine learning and or AI could be applied to this model to allow for constraints to be input and the optimal system output and behavior to be found more easily. Measurement of safety risks should be considered essential to add to this model as strong magnetic fields can be detrimental to human and animal health. A few modifications can be made to the simulation and script to increase simulation speed and decrease resource intensity. Half of the mutual inductance curve could be calculated, copied, and reflected to create the full mutual inductance curve if the receiving coil's path is straight over the system's span. Suppose the transmitting coils are identical, adequately spaced, and the receiving coil moves along a straight path. In that case, the system could be reduced to the output of a single coil system multiplied by the number of transmitting coils to approximate the system as long all other factors are held constant. The next step for this model would be to modify it to apply to more possible situations.

The most impactful modification that could be made is modifying the code for multiple receiving coils and consider what happens when a device is coupled to more than one

transmitting coil or more than one device is coupled to a transmitting coil. Both situations would occur on a busy highway. It is also paramount to look into how to model this system using renewable energy sources. One possibility for increased power transfer capability and efficiency would be to use self-resonant coils, which would remove the need for a compensating capacitor and decrease the unit's package size and overall cost [18]. However, this is difficult as the frequency for self-resonance is generally restrictively high. Load balancing, unity corrections, and other power electronic strategies could also be applied to the system. A few simple modifications could be made to the existing model to change the constant velocity to a variable velocity and change the receiving coil's path and or layout of the transmitting coils from a straight path to a variable path.

REFERENCES

- [1] Laboratory for Atmospheric Space Physics, "Solar Radiation Diagram," University of Colorado Boulder, 2020. [Online]. Available: https://lasp.colorado.edu/home/education/k-12/climate-change-compendium/photo-gallery/d1/?doing_wp_cron=1456858815.3361930847167968750000. [Accessed 17 02 2019].
- [2] D. A. Lashof and D. R. Ahuja, "Relative Contributions of Greenhouse Gas Emissions to Global Warming," *Letters to Nature*, vol. 344, pp. 529-531, 1990.
- [3] Global Carbon Atlas, "Carbon Story-Present-Visualizing human impact," Fondation BNP Paribas, [Online]. Available: <http://globalcarbonatlas.org/en/outreach>. [Accessed 20 8 2020].
- [4] F. Ackerman, E. A. Stanton, C. Hope and S. Alberth, "The Cost of Climate Change: What We'll Pay of Global Warming Continues Unchecked," Natural Resource Defense Council, Inc., New York, 2008.
- [5] US Environmental Protection Agency, "Green House Gas Emissions," US Environmental Protection Agency, 2018. [Online]. Available: <http://www.epa.gov/ghgemissions/sources-greenhouse-gas-emissions>. [Accessed 19 02 2019].
- [6] F. Deflorio, P. Guglielmi, I. Pinna, L. Castello and S. Marfull, "Modeling and Analysis of Wireless "Charge While Driving" Operations for Full Electric Vehicles," *Transportation Research Procedia*, vol. 5, pp. 161-174, 2015.
- [7] P. M. S. M. Rodrigues, A. M. M. C. Antão and R. Rodrigues, "Evaluation of the impact of lithium exploitation at the C57 mine (Gonçalo, Portugal) on water, soil and air quality," *Environmental Earth Sciences*, vol. 78, 2019.
- [8] U.S. Energy Information Administration, "Electricity Data Browser," U.S. Energy Information Administration, 10 2020. [Online]. Available: <https://www.eia.gov/electricity/data/browser/>. [Accessed 01 10 2020].
- [9] U.S. Energy Information Administration, "How much carbon dioxide is produced when different fuels are burned?," U.S. Energy Information Administration, [Online]. Available: <https://www.eia.gov/tools/faqs/faq.php?id=73&t=11>. [Accessed 12 06 2020].
- [10] Efficient Power Conversion Corporation, "Overview of Wireless Power Transfer," in *EPC Wireless Power Handbook*, Efficient Power Conversion Corporation, 2015, pp. 1-7.

- [11] SAE International, "SAE International Publishes Two New Documents Enabling Commercialization of Wireless Charging for Electric Vehicles," SAE International, 22 10 2020. [Online]. Available: <https://www.sae.org/news/press-room/2020/10/sae-international-publishes-two-new-documents-enabling-commercialization-of-wireless-charging-for-electric-vehicles#.X5GO28lJ3a0.twitter>. [Accessed 1 11 2020].
- [12] K. A. Kalwar, M. Aamir and S. Mekhilef, "Inductively Coupled Power Transfer (ICPT) for Electric Vehicle Charging- A Review," *Renewable and Sustainable Energy Reviews*, vol. 47, p. 462–475, 2015.
- [13] O. C. Onar, J. M. Miller, S. L. Campbell, C. Coomer, C. P. White and L. E. Seiber, "A novel wireless power transfer for in-motion EV/PHEV charging," in *IEEE Applied Power Electronics Conference and Exposition (APEC)*, Long Beach, 2013.
- [14] J. M. Miller, P. T. Jones, J.-M. Li and O. C. Onar, "ORNL Experience and Challenges Facing Dynamic Wireless Power Charging of EV's," *IEEE Circuits and Systems Magazine*, vol. 15, no. 2, pp. 40-53, 2015.
- [15] "Tesla flat spiral coil," Coil32, 9 January 2015. [Online]. Available: <https://coil32.net/online-calculators/flat-spiral-pancake-tesla-coil.html>. [Accessed 19 March 2020].
- [16] R. C. Dorf and R. H. Bishop, "State Variable Models," in *Modern Control Systems*, 11 ed., Upper Saddle River, NJ: Pearson Prentice Hall, 2008, pp. 144-211.
- [17] S. Liu, J. Su and J. Lai, "Accurate Expressions of Mutual Inductance and Their Calculation of Archimedean Spiral Coils," *MDPI Energies*, vol. 12, no. 10, pp. 2017-2031, 2019.
- [18] D. Clark, "Considerations When Designing a Wireless Charging System," Abracon, Spicewood, 2018.

APPENDICES

Appendix A Source Code

```
% =====
% =====
% Filename: System_Parameters_and_LM_Calc
% Author: Joshua Turnbull
% Date Created: 02/10/2020
% Date Last Modified: 11/08/2020
% Thesis Code
%
% Description:
% This code is meant to take the physical parameters of a receiving coil,
% one or more transmitting coils, and the rest of the system. This code is
% an accurate approximation given there is sufficient spacing between the
% transmitting coils. Meaning the transmitting coils are spaced far enough
% apart so that at no point in time is the receiving coil coupled to more
% than one transmitting coil. Essentially the systems are separate. The
% greater the resolution, the more time it will take, but the spline will be
% more accurate. The Attached Simulink® simulation needs to have twice the
% PPC per cycle to fulfill Nyquist-Shannon-Sampling Theorem. The calculated
% mutual inductance points are placed into a spline, which the simulation
% uses to query at each time step.
%=====
%=====

% overall system and calculate the mutual inductance between
% =====

tic %Start the stopwatch

%Initialization of Transfer Coil Parameters
% =====
NumCoil=1; %Number of Transmitting Coils
OR_p=0.75; %Transfer Coil Outer Radius (meters)
IR_p=0.017526; %Transfer Coil Inner Radius (meters)
n_p=22; %Number of turns for Primary Coil
Rp=0.0094872; %Transfer Coil Resistance (Ohms)
Lp=0.0002; %Transfer Coil Inductance (Henry)
Cp=1.407239E-09; %Capacitor in Transfer Coil Circuit (Farad)

%Initialization of Receiving Coil Parameters
% =====
OR_s=0.75; %Receiving Coil Outer Radius (meters)
IR_s=0.017526; %Receiving Coil Inner Radius (meters)
n_s=22; %Number of turns for Secondary Coil
Rs=0.0094872; %Receiving Coil Resistance (Ohms)
Ls=0.0002; %Receiving Coil Inductance (Henry)
Cs=1.407239E-09; %Capacitor in Receiving Coil Circuit (Farad)
```

```

%Initialization of Circuit and Simulation Parameters
% =====
mu=1.25663753e-6;                                     %Magnetic Permeability of air
f=300000;                                              %Resonance Frequency (Hz)
w=2*pi*f;                                            %For ease of formulas using w
V_in=120;                                             %Voltage Input (Volts)
velocity=26.8224;                                       %Velocity (m/s)
RL=100;                                                %Load Resistance (Ohm)
PPC=25;                                                 %Points per Coil
PR=(OR_p^2)/PPC;                                       %Frequency an LM point is taken
h=3;                                                    %Height(meters)
Spacing=30;                                            %Space between TCs
TD=NumCoil*Spacing+(NumCoil*(OR_p^2));                %Total Distance traveled
Resolution=TD/PR;                                       %Data points taken for the LM
t_end=TD/velocity;                                     %Duration of the Simulation (s)

%Initialization of Parameters for Mutual Inductance Calculation
% =====
S_p=(OR_p-IR_p)/n_p;                                  %Screw Pitch Formula solved for Transfer Coil
S_s=(OR_s-IR_s)/n_s;                                  %Screw Pitch Formula solved for Receiver Coil
a_p=S_p/(2*pi);                                       %Divides Screw Pitch by a full rotation
a_s=S_s/(2*pi);                                       %Divides Screw Pitch by a full rotation
Phi_i_p=IR_p/a_p;                                     %Calculates xmin Phi ID1 bound
Phi_o_p=OR_p/a_p;                                     %Calculates xmax Phi OD1 bound
Phi_i_s=IR_s/a_s;                                     %Calculates ymin Phi ID2 bound
Phi_o_s=OR_s/a_s;                                     %Calculates ymax Phi OD2 bound
M_Table=ones(1,Resolution);                           %Initialize the Mutual Inductance Table

%Placement of the Transfer Coils
% =====
x_p=ones(1,NumCoil);                                 %X values of Transfer Coil centers
y_p=0;                                                 %Straight line TC centers on "X-Axis"
z_p=0;                                                 %TCs are on flat ground at ground level

for i=1:1:NumCoil
x_p(1,i)=((2*i-1)*OR_p)+((i-0.5)*Spacing);    %Graph starts with half spacing
end

%Path of the Receiving Coil (RC)
% =====
y_s=0;                                                 %Off centered straight line path
x_s=ones(1,Resolution);                            %X values of Receiving coil centers
step=t_end/Resolution;                            %Step size for the time values
t_s=0:step:t_end-step;                           %Query points for spline function
z_s=h;

for j=1:1:Resolution
x_s(1,j)=velocity*t_s(1,j); %X-Value of Center of RC
end

%Calculation of M_Table for two Coils
%=====
for u=1:1:525                                     %Defines the function at each point
polarfun=@(phi1,phi2) ((cos(phi1)-phi1.*sin(phi1)).*...
(cos(phi2)-phi2.*sin(phi2))+(sin(phi1)+phi1.*cos(phi1)).*...
(sin(phi2)+phi2.*cos(phi2)))./(sqrt(((x_s(1,u)+a_s*phi2.*...

```

```

cos(phi2)-(x_p(1,1)+a_p*phil.*cos(phi1)).^2+((y_s+a_s*phi2.*...
sin(phi2))-(y_p+a_p*phil.*sin(phi1))).^2+(z_s)^2);

M_Table(1,u)=integral2(polarfun,Phi_i_p,Phi_o_p,Phi_i_s,Phi_o_s, ...
'Method','iterated'); %Double integral
end

% Calculate the Mutual Inductance of a Second Transmitting Coil (TC2)
%=====
% for b=526:1:1050
%     polarfun=@(phil,phi2)((cos(phi1)-phil.*sin(phi1)).*...
%     (cos(phi2)-phi2.*sin(phi2))+(sin(phi1)+phil.*cos(phi1)).*...
%     (sin(phi2)+phi2.*cos(phi2))./(sqrt(((x_s(1,b)+a_s*phi2.*...
%     cos(phi2))-(x_p(1,1)+a_p*phil.*cos(phi1)).^2+((y_s+a_s*phi2.*...
%     sin(phi2))-(y_p+a_p*phil.*sin(phi1))).^2+(z_s)^2));
%
% M_Table(1,b)=integral2(polarfun,Phi_i_p,Phi_o_p,Phi_i_s,Phi_o_s, ...
% 'Method','iterated'); %Does the double integral
% end

% Plot Mutual Inductance and Coil Position
%=====

plot(t_s,M_Table)
hold on
xline((x_p(1,1)/velocity),'--r') %Center of the TC1
xline(((x_p(1,1)-OR_p)/velocity),'--k') %Plots the left edge of TC1
xline(((x_p(1,1)+OR_p)/velocity),'--k') %Plots the right edge of TC1

% Plot the Location of a Second Transmitting Coil (TC2)
%=====
% xline((x_p(1,2)/velocity),'--r') %Center of the TC2
% xline(((x_p(1,2)-OR_p)/velocity),'--k') %Plots the left edge of TC2
% xline(((x_p(1,2)+OR_p)/velocity),'--k') %Plots the right edge of TC2
hold off

toc %End the stopwatch

```

Appendix B Example of Excel Calculation Sheet

30m, Identical Coil, 1 Transmitting Coil Simulation			
Parameters Half Space First		Formulas for the coil layouts	
# Transmitting Coils (#TC)	1	Setup	Distance
Spacing (Sp)	30	Transmitting Coil First	$((2*i-1)*OR_p)+((i-1)*Spacing)$
Speed (Vel)	26.8224	Space First	$((2*i-1)*OR_p)+(i*Spacing)$
Transmitting Coil Diameter (TCD)	1.5	Half Space First	$((2*i-1)*OR_p)+((i-0.5)*Spacing)$
Total Distance (TD)	$(B3)*B4+B3*B6$		
t_end	B7/B5	Formulas for Total Distance	
Points per M Curve	25	Setup	Distance
Point Resolution	B6/B9	Transmitting Coil First	$Sp * #TC + #TC * TCD$
Number of points (Resolution)	B7/B10	Space First	$(#TC + 1) * Sp + #TC * TCD$
		Half Space First	$(#TC) * Sp + #TC * TCD$
Coil Parameters			
	Transmitter	Receiver	
Outer Diameter	1.5	1.5	
Inner Diameter	0.0234	0.0234	
Turns	22	22	
R	M16*0.0001608	N16*0.0001608	
L	0.0002	0.0002	
C	$((1/(2*\pi*$M5))^2)/M14$	$((1/(2*\pi*$M5))^2)/N14$	
Length	59	59	
Default Values are			
Variable	Value	Unit	
Magnetic Permeability (μ_0)	1.25664E-06	H/m	
V_In	120	V	
Frequency	300000Hz	Hz	
Speed	26.8224	m/s	
Y_Offset	0	m	
Z_Offset	0.1778	m	
RL	100	Ω	
Spacing	30	m	
Points Per Coil	25	Unitless	
Simulation Points Per Cycle	50	Unitless	

Appendix C Output Energy Values for Identical Coils

Identical Coil Output Power Values				
Variable	Value (Hz)	kHz	Output (Ws)	kWS
Freq	100000	100	1.5546E-04	1.5546E-07
	200000	200	0.0989	9.8913E-05
	300000	300	34931.5072	34.9315
	400000	400	1.3712	1.3712E-03
	500000	500	1.3308	1.3308E-03
Variable	Value (m/s)	Output (Ws)	kWS	
Speed	8.9408	90923.1695	90.9232	
	15.6464	54211.7702	54.2118	
	20.1168	43745.1335	43.7451	
	26.8224	34931.5072	34.9315	
	31.2928	31307.7426	31.3077	
Variable	Value (Ω)	Output (Ws)	kWS	
RL	0.01	35897.9512	35.8980	
	0.1	62488.8364	62.4888	
	1	57609.8951	57.6099	
	10	45454.2374	45.4542	
	100	34931.5072	34.9315	
Variable	Value (m)	Output (Ws)	kWS	
Y Offset	0	34931.5072	34.9315	
	0.375	35157.1039	35.1571	
	0.75	36046.9604	36.0470	
	1.5	38523.2228	38.5232	
	3	48819.3624	48.8194	
Variable	Value (m)	Output (Ws)	kWS	
Z Offset	0.1778	34931.5072	34.9315	
	0.375	36298.6493	36.2986	
	0.75	43812.4353	43.8124	
	1.5	27864.0688	27.8641	
	3	37410.1378	37.4101	

Appendix D Output Energy Values for Non-Identical Coils

Non-Identical Coil Output Energy Values				
Variable	Value (Hz)	kHz	Output (Ws)	kWS
Freq	100000	100	2.2656E-04	2.2656E-07
	200000	200	0.0211	2.1099E-05
	300000	300	24188.3191	24.1883
	400000	400	0.1922	1.9216E-04
	500000	500	0.0812	8.1220E-05
Variable	Value (m/s)	Output (Ws)	kWS	
Speed	8.9408	53028.5577	53.0286	
	15.6464	33727.6007	33.7276	
	20.1168	28469.1093	28.4691	
	26.8224	24188.3191	24.1883	
	31.2928	22481.3956	22.4814	
Variable	Value (Ω)	Output (Ws)	kWS	
RI	0.01	40459.0962	40.4591	
	0.1	39398.1534	39.3982	
	1	33667.9112	33.6679	
	10	27840.6944	27.8407	
	100	24188.3191	24.1883	
Variable	Value (m)	Output (Ws)	kWS	
Y Offset	0	24188.3191	24.1883	
	0.375	24658.7470	24.6587	
	0.75	29464.1162	29.4641	
	1.5	25083.3244	25.0833	
	3	424.3896	0.4244	
Variable	Value (m)	Output (Ws)	kWS	
Z Offset	0.1778	24188.3191	24.1883	
	0.375	27061.1154	27.0611	
	0.75	20669.6583	20.6697	
	1.5	25611.2789	25.6113	
	3	5964.2398	5.9642	